Electronic Supplementary Information

Theoretical characterization of hexagonal 2D Be_3N_2 monolayer

Saif Ullah,[a,*] Pablo A. Denis,[b] Rodrigo B. Capaz[c†], and Fernando Sato[a]

a- Departamento de Física, Instituto de Ciências Exatas, Campus Universitário, Universidade Federal de Juiz de Fora, Juiz de Fora, MG 36036-900, Brazil

b- Computational Nanotechnology, DETEMA, Facultad de Química, UDELAR, CC 1157, 11800 Montevideo, Uruguay

c- Instituto de Física, Universidade Federal do Rio de Janeiro, Caixa Postal 68528, Rio de Janeiro, RJ 21941-972, Brazil

*email: sullah@fisica.ufjf.br

†email: capaz@if.ufrj.br

Computational details:

We make use of four DFT codes i.e. VASP[1], QE[2, 3], SIESTA[4, 5], and Gaussian[6] to predict the theoretical synthesis, stability, and electronic properties of Be_3N_2 and its derivatives. We use norm-conserving (NC) Troullier-Martins pseudopotentials (PPs)[7] in SIESTA. We use LDA[8], PBE-GGA[9], LDA-PBE hybrid, vdW-DF1[10], and vdW-DF2-C09[11, 12] as implemented in SIESTA. The hybrid functional is actually not a hybrid in a true sense due to the absence of exact Hartree-Fock exchange. The term hybrid is used as we mixed two different functionals, LDA and PBE versions of GGA. We select 50-50 % from both these functionals to define the exchange energy while for correlation part, 75% and 25% is used from LDA and GGA, respectively. The orbital confining cut-off is 0.01 Ry and the split-norm is 0.15. We tested increasing the mesh cut-off to 300 Ry, which gave the same results as that of 200 Ry. For AIMD simulations, we constructed a 4x4 supercell of Be_3N_2 and performed the heat treatment at 300K, 600K, and 900K. An NVT ensemble with Nosé thermostat is used with a time step of 1 fs . In VASP, the kinetic energy cut-off is 500 eV. Geometry optimization is carried out with two different convergence criteria: 10^{-6} eV for energy and 0.02 eV/Å for forces; and 10^{-8} eV for energy and 0.0001 eV/Å for forces in some cases. Both of these criteria gave converged results. To deal with of partial occupancies,

tetrahedron method with Blochl correction[13] is used. For bulk graphite-like layered structures, we use dispersion corrected PBE-D2[14] scheme and for total energy comparison, all the systems are recalculated with the same functional. As for as QE is concerned, we use PPs from PSlibrary[15] and SSSP library[16, 17]. The cut-off is selected to be 60 Ry for the expansion of the wavefunctions (wfc) and 8-times of this cut-off is used for charge density. The default 4×wfc is selected if the PPs are NC. A smaller cutoff of 40Ry also produces well-converged results. The convergence criteria of energy (between two electronic steps) and two ionic steps are 10^{-10} Ry and 10^{-7} Ry. The optimization is done until the Hellmann-Feynman forces are less than 10^{-5} Ry/a.u. For self-consistent field convergence, we use more strict criteria of 10^{-13} Ry. We use Methfessel-Paxton (mp)[18] and Marzari-Vanderbilt (mv)[19] smearing method with 0.01-0.005Ry and found that mp smearing method with a broadening of 0.01 Ry is a wise choice in term of accuracy versus computational speed. Phonons spectra are calculated by DFPT method using the Phonon code, which is a part of PWscf package. We use PBE, PBE-sol, and NC PPs and found that all the levels employed gave the same results. In phonon calculations, the convergence criterium is selected to be 10^{-15} Ry. Furthermore, vdW-DF1, rev-vdW-DF2[20], vdW-DF2-C09 (with C-09 exchange), rVV10[21, 22] schemes are also used in QE.

All the calculations are performed with spin polarization to investigate possible magnetism. We also tested the inclusion of spin-orbit-coupling (SOC) in our calculations but no effect was noted on the electronic band structure or the total energy of Be3N2. Furthermore, we also tested antiferromagnetic calculations with various configurations. After checking all these possibilities, we can safely say that Be3N2 is a non-magnetic direct band-gap semiconductor.

DFT level	**Code**	**Lattice parameter a=b (Å)**	**Lattice parameter c (Å)**	**Be-N bond lengths (Å)**	**Cohesive energy (eV/atom)**	**Formation energy (eV)**
β-Be_3N_2						
PBE	SIESTA	2.946	10.2		-4.61	
vdW-DF/DZP	SIESTA	2.96	10.24			

PBE[a]	QE	2.77	10.21		-4.95	
PBE-sol	QE	2.829	9.68			-1.16
paw-PBE	QE	2.843	9.74		-5.4	
rVV10	QE	2.85	9.785			
vdW-DF1	QE	2.859	9.82			
vdW-DF2	QE	2.84	9.73			
rev-vdW-DF2	QE	2.834	9.71			
vdW-DF2-C09	QE	2.833	9.70			
2D Be_3N_2						
LDA	SIESTA	5.53		1.6		
PBE	SIESTA	5.53		1.6		-0.403
Hybrid	SIESTA	5.53		1.6	-4.1	
vdW-DF/DZP	SIESTA	5.55		1.61		
PBE-NC	QE	5.2		1.5		
PBE-sol	QE	5.24		1.51	-5.075	-0.512
PBE[a]	QE	5.26		1.52	-4.81	
vdW-DF1	QE	5.238		1.51		
rVV10	QE	5.269		1.52		
rev-vdW-DF2	QE	5.27		1.52		
vdW-DF2-C09	QE	5.276		1.52		
paw-LDA	QE	5.196		1.5		
LDA-NC	QE	5.128		1.48		

Table S1: *Structural properties of β-Be_3N_2 and monolayer Be_3N_2 are shown at the different level of theories.*

DFT level	Exfoliation Energy (eV/Å^2)
vdW-DF/DZP	0.13
vdW-DF1	0.09
rVV10	0.12
DF2-C09	0.15
rev-vdW-DF2	0.14

Table S2: *The Exfoliation energies for monolayer Be_3N_2 at various vdW-DF levels are shown.*

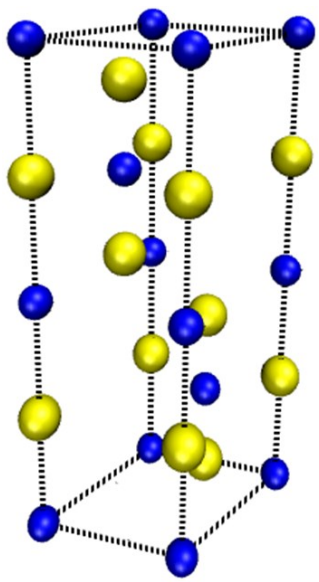

Fig. S1: *The geometric structure of bulk β-Be_3N_2 calculated at PBE-sol level of theory is depicted.*

DFT level	Code	Band-gap (eV)
LDA	SIESTA	2.78
PBE	SIESTA	2.86
Hybrid	SIESTA	2.76
vdW-DF/DZP	SIESTA	2.76
vdW-DF/DZP-SOC	SIESTA	2.76
PBE	QE	2.82

PBE-sol	QE	2.77
HSEH1PBE	Gaussian	4.10

Table S3: *Calculated band-gaps of monolayer Be3N2 at various levels of theory.*

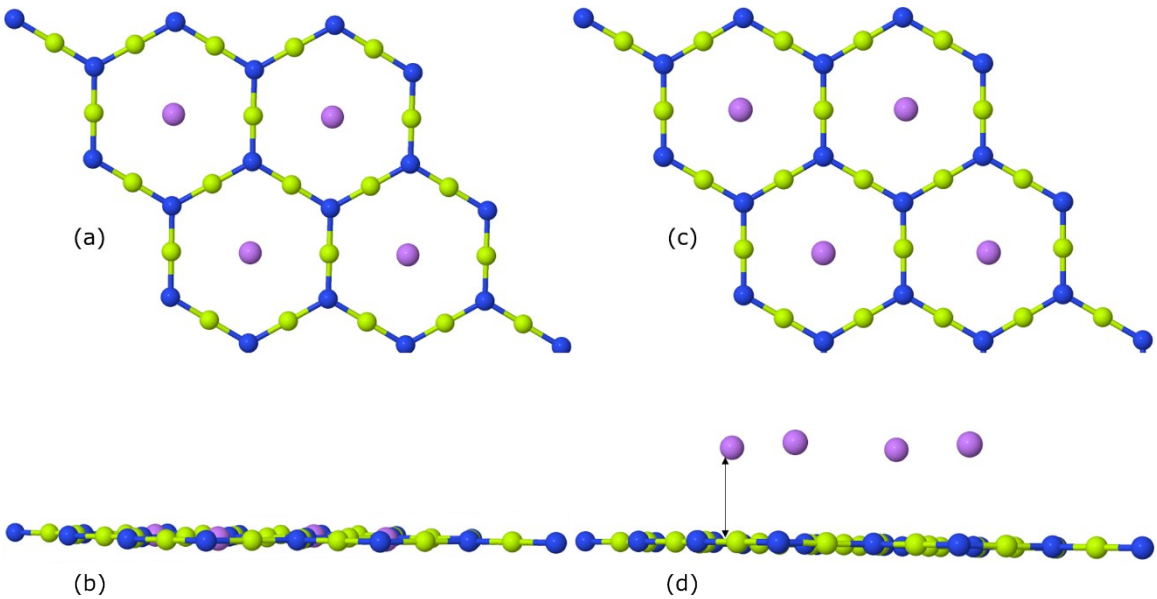

Fig. S2: *Alkali atoms (Li, Na, and K) adsorbed within the hollow site (a) top view (b) side view and on the top of hollow site (c) top view (d) side view) on monolayer Be_3N_2. In the latter case, the height of Li, Na, and K from the plane of monolayer Be_3N_2 is found to be 3.209 Å, 2.767 Å, and 3.153 Å, respectively.*

Branch	Frequency (THz)	Infrared (I)-Active	Raman-R-Active	depol-fact
1	0	0	0	0.3931
2	0	0	0	0.664
3	0	0	0	0.7495
4	4.675	0	0	0.75
5	8.7431	0	0	0.75
6	9.0271	0	0	0.75
7	9.0271	0	0	0.75
8	14.3784	1.8474	0	0.75
9	15.8432	1.6547	0	0.75
10	15.8442	1.6535	0	0.2264
11	26.057	0	0.3638	0.7498
12	26.0582	0	0.3651	0.75
13	36.9998	0	0	0.4827
14	40.3884	40.527	0	0.75
15	40.3899	40.533	0	0.1315

Table S4: *There are three IR active modes and one Raman active mode. The IR and Raman data along with results of phonon calculated at gamma point shown in the table to expedite the experiment.*

References:

1. G. kresse and J. Hafner, *Phys. Rev. B*, 1994, **49**, 14251.
2. P. Giannozzi, S. Baroni, N. Bonini, M. Calandra, R. Car, C. Cavazzoni, D. Ceresoli, G. L. Chiarotti, M. Cococcioni and I. Dabo, *Journal of physics: Condensed matter*, 2009, **21**, 395502.
3. P. Giannozzi, O. Andreussi, T. Brumme, O. Bunau, M. B. Nardelli, M. Calandra, R. Car, C. Cavazzoni, D. Ceresoli and M. Cococcioni, *Journal of Physics: Condensed Matter*, 2017, **29**, 465901.
4. P. Ordejón, E. Artacho and J. M. Soler, *Physical Review B*, 1996, **53**, R10441-R10444.
5. J. M. Soler, E. Artacho, J. D. Gale, A. Garcia, J. Junquera, P. Ordejon and D. Sanchez-Portal, *J. Phys.: Condens. Matter*, 2002, **14**, 2745.
6. M. Frisch, G. Trucks, H. Schlegel, G. Scuseria, M. Robb, J. Cheeseman, G. Scalmani, V. Barone, B. Mennucci and G. Petersson, *Journal*, 2009.
7. N. Troullier and J. L. Martins, *Physical Review B*, 1991, **43**, 1993-2006.
8. J. P. Perdew and A. Zunger, *Physical Review B*, 1981, **23**, 5048-5079.
9. J. P. Perdew, K. Burke and M. Ernzerhof, *Physical review letters*, 1996, **77**, 3865.
10. M. Dion, H. Rydberg, E. Schröder, D. C. Langreth and B. I. Lundqvist, *Physical Review Letters*, 2004, **92**, 246401.
11. K. Lee, É. D. Murray, L. Kong, B. I. Lundqvist and D. C. Langreth, *Physical Review B*, 2010, **82**, 081101.
12. V. R. Cooper, *Physical Review B*, 2010, **81**, 161104.
13. P. E. Blöchl, O. Jepsen and O. K. Andersen, *Physical Review B*, 1994, **49**, 16223-16233.
14. S. Grimme, *Journal of computational chemistry*, 2006, **27**, 1787-1799.
15. A. Dal Corso, *Computational Materials Science*, 2014, **95**, 337-350.
16. G. Prandini, A. Marrazzo, I. E. Castelli, N. Mounet and N. Marzari, 2018.
17. D. Hamann, *Physical Review B*, 2013, **88**, 085117.
18. M. Methfessel and A. T. Paxton, *Physical Review B*, 1989, **40**, 3616-3621.
19. N. Marzari, D. Vanderbilt, A. De Vita and M. C. Payne, *Physical review letters*, 1999, **82**, 3296-3299.
20. I. Hamada, *Physical Review B*, 2014, **89**, 121103.
21. O. A. Vydrov and T. Van Voorhis, *Physical review letters*, 2009, **103**, 063004.
22. R. Sabatini, T. Gorni and S. de Gironcoli, *Physical Review B*, 2013, **87**, 041108.